Environ Sci Pollut Res (2013) 20:6210–6221
DOI 10.1007/s11356-013-1651-8

RESEARCH ARTICLE

Cadmium (Cd^{2+}) removal by nano zerovalent iron: surface analysis, effects of solution chemistry and surface complexation modeling

Hardiljeet K. Boparai · Meera Joseph · Denis M. O'Carroll

Received: 15 January 2013 / Accepted: 15 March 2013 / Published online: 16 April 2013

Abstract Nano zerovalent iron (nZVI) is an effective remediant for removing various organic and inorganic pollutants from contaminated water sources. Batch experiments were conducted to characterize the nZVI surface and to investigate the effects of various solution properties such as pH, initial cadmium concentration, sorbent dosage, ionic strength, and competitive ions on cadmium removal by nZVI. Energy-dispersive X-ray and X-ray photoelectron spectroscopy results confirmed removal of Cd^{2+} ions by nZVI through adsorption. Cd^{2+} adsorption decreased in the presence of competitive cations in the order: $Zn^{2+}>Co^{2+}>Mg^{2+}>Mn^{2+}=Cu^{2+}>Ca^{2+}>Na^{2+}=K^{+}$. Higher concentrations of Cl^{-} significantly decreased the adsorption. Cadmium removal increased with solution pH and reached a maximum at pH 8.0. The effects of various solution properties indicated Cd^{2+} adsorption on nZVI to be a chemisorption (inner-sphere complexation) process. The three surface complexation models (diffuse layer model, constant capacitance model, and triple layer model) fitted well to the adsorption edge experimental data indicating the formation of nZVI–Cd bidentate inner-sphere surface complexes. Our results suggest that nZVI can be effectively used for the removal of cadmium from contaminated water sources with varying chemical conditions.

Keywords Cadmium · Adsorption · Nano zerovalent iron · pH · Competitive cations · Ionic strength · Surface complexation modeling

Responsible editor: Philippe Garrigues

H. K. Boparai (✉) · M. Joseph · D. M. O'Carroll
Department of Civil and Environmental Engineering,
Faculty of Engineering, The University of Western Ontario,
1151 Richmond St. N,
London, ON N6A 5B9, Canada
e-mail: hboparai@uwo.ca

Introduction

Cadmium is a potent carcinogen causing damage to the lungs, kidneys, liver, and reproductive organs (Zalups and Ahmad 2003). As a result, there is considerable interest in removing cadmium from contaminated sites before it reaches drinking water sources. It is released into the environment either from natural sources such as volcanic eruptions and forest fires or from anthropogenic activities such as non-ferrous metals production, electroplating, manufacturing of Ni-Cd batteries and pigments, application of phosphatic fertilizers, and burning of fossil fuels (Dinis and Fiuza 2011). This has resulted in serious contamination of soil and water. Cadmium has been found in at least 1,014 of the 1,669 current or former National Priorities List sites in the USA (ATSDR 2008) and is ranked as the seventh most important hazardous substance in the USA (ATSDR 2011).

Adsorption has been developed as a simple, efficient, and cost-effective treatment for removing heavy metals. A number of adsorbents have been used for cadmium removal including biopolymers, activated carbon, metal oxides, clays, dried plant parts, microorganisms, and sewage sludge (Benguella and Benaissa 2002; Huang et al. 2005; Kumar et al. 2010; Mohapatra et al. 2010; Moreno-Castilla et al. 2004; Soltani et al. 2009; Unuabonah et al. 2008). Nano zerovalent iron (nZVI), with a higher adsorption capacity, has been found to be the most effective adsorbent for removing Cd^{2+} from aqueous solutions in comparison to a variety of adsorbents (Table 1). nZVI has been identified as having significant potential for environmental applications due to its extremely small particle size, large surface area, and greater density of reactive and adsorptive sites. Nano iron technology is being successfully applied to treat various organic and inorganic contaminants (e.g., Kanel et al. 2006; Li and Zhang 2007; Petersen et al. 2012; Sakulchaicharoen et al. 2010; Satapanajaru et al. 2008; Xi et al. 2010).

Table 1 Comparison of Cd^{2+} adsorption capacities of various adsorbents

Adsorbent	Adsorption capacity (mmol g^{-1})	Reference
Chitin	0.144	(Benguella and Benaissa 2002)
Granular activated carbon	0.090	(Moreno-Castilla et al. 2004)
Dried activated sludge	1.815	(Soltani et al. 2009)
Bacteria	0.171	(Huang et al. 2005)
Rice husk	0.189	(Kumar et al. 2010)
Ficus religiosa leaf powder	0.241	(Rao et al. 2011)
Modified kaolinite clay	0.392	(Unuabonah et al. 2008)
Nanostructured goethite	0.259	(Mohapatra et al. 2010)
nZVI	6.84	(Boparai et al. 2011)

The efficiency of nZVI to remove metal ions is strongly affected by solution properties including pH, initial metal concentration, nZVI dosage, and the presence of competitive ions. pH influences metal sorption onto nZVI by both controlling the formation of an outer iron oxide layer as well as changing the surface charge (Kanel et al. 2005). Various ions (e.g., Ca^{2+}, Na^{+}, Mg^{2+}, Cl^{-}, PO_4^{3-}, HCO_3^{-}) commonly present in water sources as well as the heavy metals existing as co-contaminants at mixed waste sites may also compete with each other for the adsorption sites. Although research has investigated the factors and mechanisms influencing removal of redox-sensitive metals (e.g., As, Cr, U, Se, Ni, Cu) by nZVI, comparatively little research has studied the metals (e.g., Zn, Cd, Ba) which are removed mainly by adsorption onto nZVI (O'Carroll et al. 2012). Mondal et al. (2004) reported a significant decrease in selenate removal with increasing pH, whereas the uptake of Co^{2+} increased from 15 to 99 % with an increase in pH from 4 to 10 (Üzüm et al. 2008). Efecan et al. (2009) did not notice any change in Ni^{2+} uptake with increasing pH at high nZVI loadings. Thus, metal removal by nZVI may decrease or increase with pH depending upon the ionic form and the removal mechanism of the metal contaminant. Among various anions studied, HCO_3^{-} and PO_4^{3-} greatly reduced the uptake of As^{3+} and As^{5+} by nZVI (Kanel et al. 2006, 2005). Similarly, Yan et al. (2010) reported about 80 % decrease in U^{6+} removal when HCO_3^{-} or Ca^{2+} concentrations were increased from 0 to 1 mM. While studying the effects of various solution properties on Cd^{2+} removal by nZVI, Efecan (2008) used very high doses of nZVI (2.5 to 10 g L^{-1}) and did not find any effects of nZVI loading, pH, and competitive cations on Cd^{2+} removal. Further work is needed to assess if factors such as nZVI loading, initial Cd^{2+} concentration, pH, and competitive ions impact Cd^{2+} removal at lower nZVI doses that are more representative of concentrations at field sites. Moreover, careful monitoring and adjustment of pH is required during experiments studying the effect of pH on metal adsorption. Due to the continuous release of OH^{-} ions during the reaction between Fe^0 and H_2O, pH increases with time to ~8.0 even if the initial pH is lowered with an acid (e.g., HCl, HNO_3), as was the case with Efecan (2008). Past research has studied various adsorption and kinetic models to describe metal adsorption on nZVI surface (e.g., Boparai et al. 2011; Celebi et al. 2007; Kanel et al. 2005), but to our knowledge, this study represents the first attempt to study surface complexation models for metal adsorption on nZVI.

Previous studies have shown that factors like pH, initial Cd concentration, competitive ions, and ionic strength affect the Cd^{2+} adsorption for a variety of adsorbents (Balistrieri and Murray 1982; Benguella and Benaissa 2002; Kumar et al. 2010; Moreno-Castilla et al. 2004; Unuabonah et al. 2008). It is important to assess the effects of various solution properties on Cd removal by nZVI for the design of optimal treatment units for heavy metal removal by nZVI. The objectives of this research are to (1) characterize nZVI and cadmium adsorbed nZVI (Cd-nZVI) using spectroscopic and microscopic techniques; (2) to investigate the effects of nZVI loading, initial Cd^{2+} concentration, pH, competing ions, and ionic strength; and (3) to assess the ability of surface complexation models to describe cadmium adsorption on nZVI.

Materials and methods

Synthesis of nZVI particles

nZVI particles were synthesized in the laboratory via the following reaction:

$$4Fe^{3+} + 3BH_4^{-} + 9H_2O \rightarrow 4Fe^0 \downarrow + 3H_2BO_3^{-} + 12H^{+} + 6H_2 \uparrow \quad (1)$$

where freshly prepared $NaBH_4$ (0.125 M) was added dropwise to $FeCl_3$ (0.023 M) solution at 1:1 volume ratio with continuous stirring. Excess borohydride was added to accelerate nZVI synthesis and ensure uniform particle formation as suggested by Zhang (2003).

Black nZVI particles started appearing after adding the first few drops of borohydride solution. After the addition of $NaBH_4$ solution, the mixture was stirred continuously for an additional 20 min. The synthesis process was carried out in an anaerobic glove box maintaining an O_2-free environment by purging with O_2-free Ar (95 % Ar:5 % H_2). Deionized deoxygenated water purged with pure N_2 gas was used to prepare aqueous solutions.

Characterization of nZVI

The surface morphology of nZVI particles was characterized by a scanning electron microscope (SEM, Hitachi S-2600 N, 5 kV) with energy-dispersive X-ray (EDX). The solid samples were sprinkled onto an adhesive carbon tape supported on a metallic disk. EDX mapping was performed at randomly selected areas on the solid surfaces to show the atomic distribution on the surface of nZVI particles. The particle size distribution for nZVI particles was studied by obtaining a representative set of micrographs for the nZVI sample and measuring the diameter of each particle on those micrographs using the Quartz PCI Imaging software. Surface analysis of nZVI was also performed using Kratos Axis Ultra X-ray Photoelectron Spectroscopy (XPS, Monochromatic Al Kα X-ray source, 14 kV) to determine the elemental composition and the chemical state of the atoms present on the nZVI surface. The XPS survey scans were collected using the following parameters: pass energy=160 eV, an energy step size=0.7 eV, x-ray spot size=0.7×0.4 mm, binding energy range=1,100–0 eV, sweep time=180 s, and the number of sweeps=8 (Grosvenor et al. 2004a). High-resolution spectra were taken for Cd 3d, O 1 s, and Fe 2p using a 40–20 eV window, depending on the element being examined, and a pass energy of 20 eV. All samples were prepared and introduced into the spectrometer via an anaerobic glove box to prevent oxidation. The XPS spectra were analyzed using CasaXPS software (Fairley 1999). All spectra were calibrated using the adventitious C 1 s peak at 284.8 eV.

Cadmium adsorption by nZVI

Batch adsorption experiments were carried out in 60-mL glass vials by agitating a known amount of nZVI with 60 mL of Cd^{2+} solution at room temperature. The glass vials were capped with Teflon Mininert valves to minimize oxidation of nZVI. To study the effect of nZVI loading, 0.1–5.0 g L^{-1} nZVI was added to the reactor vials to treat 1.0 mM Cd^{2+} solution at pH 8.0. The effect of initial Cd concentration was investigated by varying the Cd concentration from 0.25 to 4.0 mM and reacting with 0.5 g L^{-1} nZVI at pH 8.0. All the experiments were performed with a background electrolyte of 0.001 M $NaNO_3$. The samples were collected at pre-defined intervals to quantify Cd concentration with time.

To study the effect of pH, experiments were conducted by adjusting the pH of the system with 0.1 M HCl or NaOH. The adsorption results showed ~100 % Cd removal by nZVI at initial pH values ranging from 4.0 to 10.0. A similar trend was reported by Efecan (2008) for removal of Ni^{2+} and Cd^{2+} by nZVI. Adding 0.1 M HCl decreased the pH of nZVI suspension for a limited time (i.e., <3 h) after which the pH rose back to ~8.0. An acid needs to be added at regular intervals to maintain low pH in the nZVI suspension (Zhu et al. 2010). As such, the pH of the nZVI suspension was controlled with a 0.02-M buffer by adjusting its initial pH with HCl or NaOH. The buffers used were acetate (sodium acetate trihydrate and acetic acid, pH ≤5.0), MES (2-(N-morpholino)ethanesulfonic acid, pH 5.5–6.0), PIPES (1,4-piperazinediethanesulfonic acid, pH 6.2–7.4), HEPES (4-(2-hydroxyethyl)-piperazine-1-ethanesulfonic acid, pH 7.5–8.2), and CHES (2-(N-Cyclohexylamino)ethanesulfonic acid, pH >8.5). These buffers have been used in previous studies with nZVI (Song and Carraway 2005), and they do not bind to metal ions (Good and Izawa 1972). Control experiments did not show any effect of buffers on Cd solubility up to pH 8.0 after which Cd started to precipitate/hydrolyze due to alkaline conditions.

The effect of competitive cations (Ca^{2+}, Mg^{2+}, Co^{2+}, Zn^{2+}, Cu^{2+}, Mn^{2+}, Na^{+}, or K^{+}) was investigated by adding 1.0 mM of a cation to the reactor vial containing 0.5 g L^{-1} nZVI and 1.0 mM Cd^{2+} solution. The effect of ionic strength was studied by adding 0–0.1 M $NaNO_3$ or NaCl to the system keeping all the experimental conditions the same.

Sample aliquots collected were filtered with 0.2-μm syringe filters. The filtrates were diluted with nitric acid and Cd^{2+} concentrations determined by inductively coupled plasma-optical emission spectrometry (Varian Vista-PRO).

Acid–base titration of nZVI suspension

The acid–base titrations of nZVI suspensions with a solid concentration of 1.0 g L^{-1} (i.e., 0.17 g nZVI in 170 mL 0.001 M $NaNO_3$ electrolyte solution) were performed in a glove box. The nZVI suspension was continuously stirred by a propeller to keep the suspension homogeneous during the titration. The titration in the acidic direction was completed by adding 0.05 M HCl and then backtitrated by adding 0.05 M NaOH until the suspension pH reached >10, with an equilibration time of 180–240 s between two increments.

Cadmium speciation/precipitation versus pH

A theoretical speciation analysis for cadmium was conducted using Visual MINTEQ version 3.0 (Gustafsson 2011). The equilibrium constants for various cadmium hydrolysis species are given in Table 2 (Lindsay 1979).

Table 2 Parameters of the speciation and surface complexation modelling

Hydrolysis reactions	Log K
$Cd^{2+} + H_2O \rightleftharpoons CdOH^+ + H^+$	−10.10[a]
$Cd^{2+} + H_2O \rightleftharpoons Cd(OH)_2^0 + 2H^+$	−20.30[a]
$Cd^{2+} + 3H_2O \rightleftharpoons Cd(OH)_3^- + 3H^+$	−33.01[a]
$Cd^{2+} + 4H_2O \rightleftharpoons Cd(OH)_4^{2-} + 4H^+$	−47.29[a]
$2Cd^{2+} + H_2O \rightleftharpoons CdOH^{3+} + H^+$	−6.40[a]
Surface ionization reactions	
$\equiv SOH \rightleftharpoons \equiv SO^- + H^+$	−9.19
$\equiv SOH + H^+ \rightleftharpoons \equiv SOH_2^+$	6.38
Surface complexation reactions	
$Cd^{2+} + \equiv SOH \rightleftharpoons \equiv SOCd^+ + H^+$	−3.4
$Cd^{2+} + 2(\equiv SOH) \rightleftharpoons \equiv (SO)_2Cd^+ + 2H^+$	−10.2
$Cd^{2+} + \equiv SOH + H_2O \rightleftharpoons \equiv SOCdOH + 2H^+$	−13.2
Other parameters	
Surface area ($m^2\ g^{-1}$)	26.3
Surface site density (sites nm^{-2})	156.6
Inner layer capacitance (C_1, F m^{-2})	1.8
Outer layer capacitance (C_2, F m^{-2})	0.2

[a] (Lindsay 1979)

Modeling was performed using the input conditions as pH=4–14, initial cadmium concentration=1.0 mM, ionic strength=0.001 M, and temperature=24 °C. The precipitation of cadmium in aqueous solutions was also studied experimentally by using 1.0 mM Cd solution and varying pH from 5 to 11. The samples were collected at specific pH values and analyzed for Cd^{2+} concentrations.

Surface complexation modeling

Data from adsorption edge experiment were modeled with the three commonly used surface complexation models (SCM)—(1) Double layer model (DLM), (2) Constant capacitance model (CCM), and (3) Triple layer model (TLM) using Visual MINTEQ. The amphoteric ionization reactions at the surface were expressed as:

$$\equiv SOH + H^+ \rightleftharpoons \equiv SOH_2^+ \tag{2}$$

$$\equiv SOH \rightleftharpoons \equiv SO^- + H^+ \tag{3}$$

Where ≡SOH represents a surface hydroxyl group. The surface site density was set to values obtained from adsorption isotherm data. The surface ionization constants (Log K^+ or Log K^-) were determined by plotting the negative logarithm of the acidity quotients (pQ^+ or pQ^-) versus fractional ionization (α^+ or α^-) and then extrapolating pQ* to zero fractional ionization (Davis et al. 1978; Hayes et al. 1991). The acidity quotients and fractional ionization were calculated as:

$$pQ^+ = pH + \log\left(\frac{\propto_+}{1 - \propto_+}\right) \tag{4}$$

$$pQ^- = pH - \log\left(\frac{\propto_-}{1 - \propto_-}\right) \tag{5}$$

$$\propto_- = -\sigma_0/N_s \quad \text{(for a negative surface)} \tag{6}$$

$$\propto_+ = \sigma_0/N_s \quad \text{(for a positive surface)} \tag{7}$$

Surface charge, σ_o (Coulomb per square meter) was calculated from the acid–base titration data:

$$\sigma_0 = \frac{F(C_A - C_B + [OH^-] - [H^+])}{C_s S_a} \tag{8}$$

where F is Faraday's constant (96,485.34 C mol^{-1}), C_A and C_B are concentrations of acid or base after addition (moles per liter), C_s is the solids concentration (grams per liter), and S_a is the specific surface area of the solid (square meters per gram).

The adsorption of Cd^{2+} on nZVI surface was assumed to occur through following surface reactions:

$$Cd^{2+} + \equiv SOH \rightleftharpoons \equiv SOCd^+ + H^+ \tag{9}$$

$$Cd^{2+} + 2(\equiv SOH) \rightleftharpoons \equiv (SO)_2Cd + 2H^+ \tag{10}$$

$$Cd^{2+} + \equiv SOH + H_2O \rightleftharpoons \equiv SOCdOH + 2H^+ \tag{11}$$

Where ≡$SOCd^+$, ≡$(SO)_2Cd$, and ≡SOCdOH denote various types of Cd^{2+} sorbed surface sites. Based on the assumptions used in the derivation of DLM, CCM, and TLM, Eqs. (9) and (10) were used in the DLM and CCM calculations, while Eqs. (9), (10), and (11) were used in the TLM calculations. The outer capacitance, C_2, for TLM was assumed to be 0.2 F m^{-2} (Hayes et al. 1991). The inner capacitance, C_1, and the surface complexation constants for reactions (9–11) were obtained from Visual MINTEQ using the surface characteristics of nZVI given in Table 2. The best fits to the experimental adsorption data for the three models were obtained by systematically optimizing the C_1 and surface complexation constants and getting the lowest possible values of $V(Y)$. The goodness-of-fit, $V(Y)$, of each

model to the experimental data was calculated as (Dzombak and Morel 1990; Schaller et al. 2009):

$$V(Y) = \frac{\sum P, Q\left(\frac{Y}{S_Y}\right)^2}{n_\mathrm{p} \times n_R - n_\mathrm{u}} \quad (12)$$

where Y is the difference between the calculated and experimental free concentrations of Cd^{2+} for each data point P, S_Y is the standard deviation, n_p is the number of data points, n_R the number of components, R, for which both the total and free concentrations are known and n_u the number of adjustable parameters. The standard deviation, S_Y, was assumed to be equal to 5 % of the Cd^{2+} concentration in each experiment.

Results and discussion

Surface analysis of nZVI and Cd-nZVI

The shape, size, and chemical composition of nZVI particles impact their adsorption capacity and reactivity towards contaminants. To characterize these properties, SEM/EDX and XPS measurements were conducted on nZVI and Cd-nZVI particles.

SEM imaging and EDX mapping of nZVI particles

SEM images of nZVI particles are shown in Fig. 1. The nZVI particles are comprised of individual, spherical particles with particle size ranging from 20 to 200 nm and assembled in chains (Fig. 1a). Chain structure formation has been attributed to the magnetic interactions between the adjacent metal particles (Zhang and Manthiram 1997). SEM analysis of nZVI particles after Cd adsorption showed that the spherical particles with chain structures were still present but also indicated the presence of larger flocs, possibly from iron oxide formation (Fig. 1b). The particle size distribution shows that ~85 % of the nZVI particles have a diameter less than 120 nm with an average particle size of ~80 nm (Fig. 2).

The nZVI and Cd-nZVI particles were further investigated for chemical composition using SEM/EDX. The SEM image of a selected area of Cd-nZVI is illustrated in Fig. 3a, and the EDX mappings of elements Fe, Cd, and O in this area are shown in Fig. 3b–d, respectively. A small fraction of boron was also present on the Cd-nZVI particles (results not shown). Cadmium is solely distributed on the nZVI particles supporting the adsorption mechanism of cadmium removal from solution (Fig. 3c). Figure 3d shows the signal of element O and confirms the existence of oxides in the Cd-nZVI sample. The iron oxides on nZVI surface form due to the reaction of nZVI with water. EDX analysis of fresh nZVI particles indicated the presence of Fe and some B and O but did not show any Cd (data not shown).

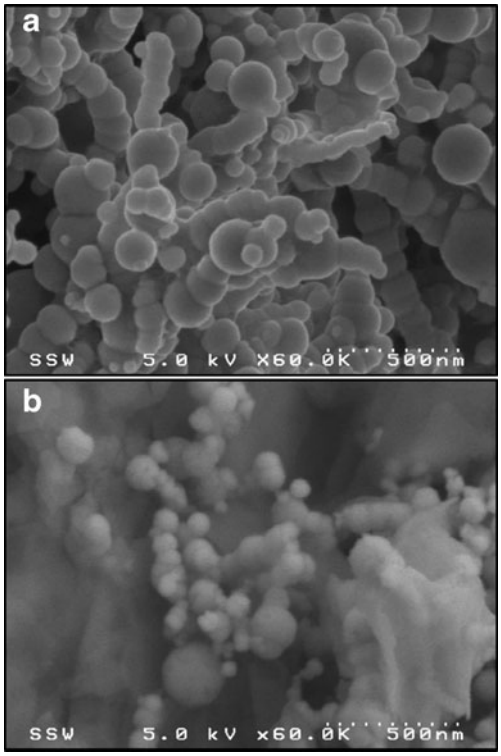

Fig. 1 SEM images of **a** fresh nZVI and **b** Cd-nZVI after 72 h of reaction

X-ray photoelectron spectroscopy

The nZVI and Cd-nZVI particles were analyzed by XPS to determine the elemental composition and the valence state of elements on the nZVI surface. The wide-scan XPS spectra of freshly prepared nZVI revealed that the nZVI surface consists mainly of iron, boron, oxygen, and carbon (Fig. 4), consistent with EDX analysis. The boron peak comes from oxidation of borohydride during nZVI synthesis. The iron peak is indicated by the Fe $2p_{3/2}$ and Fe $2p_{1/2}$ photoelectron peaks, while the oxygen peak is represented by the O 1s peak.

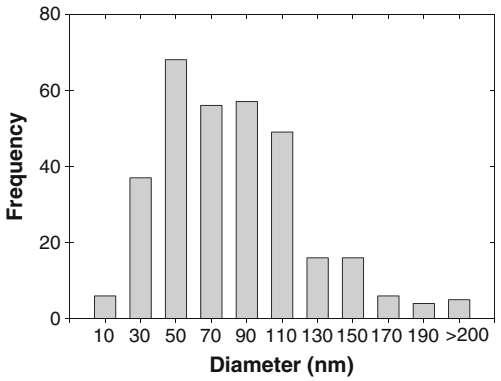

Fig. 2 Particle size distribution of nZVI particles

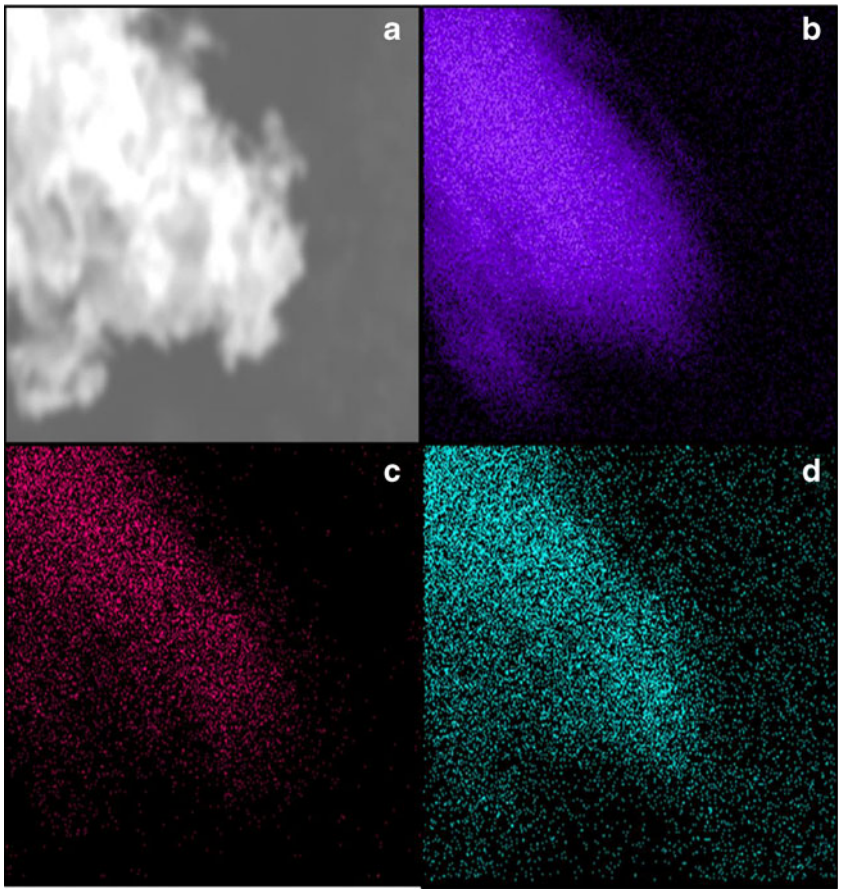

Fig. 3 **a** SEM image of a selected area of Cd-nZVI after 72 h of reaction. EDX mapping images of Cd-nZVI surface on this area: **b** Fe, **c** Cd, and **d** O

After 72-h exposure of nZVI to Cd^{2+}, an intense peak for cadmium was observed at ~405 eV (Fig. 4). The high-resolution Cd 3d spectrum of Cd-nZVI (Fig. 5a) showed photoelectron peak for Cd $3d_{5/2}$ at 405.4 which is in accordance with the values reported for Cd^{2+} in literature (Bose et al. 1989; Calareso et al. 2001). These results suggest that cadmium was removed as Cd^{2+} ions by adsorption on the nZVI surface. Depending upon the standard redox potential, the metal ions with far more positive E^0 than Fe^0 are removed by reduction, while the metals having E^0 more negative or close to that of Fe^0 are removed by sorption mechanism. The standard reduction potential of Cd^{2+} (−0.40 V, 25 °C) is very close to that of Fe^{2+} (−0.41 V, 25 °C), and thus, the removal of Cd^{2+} ions by nZVI would be expected to take place through sorption as reported earlier (Li and Zhang 2007).

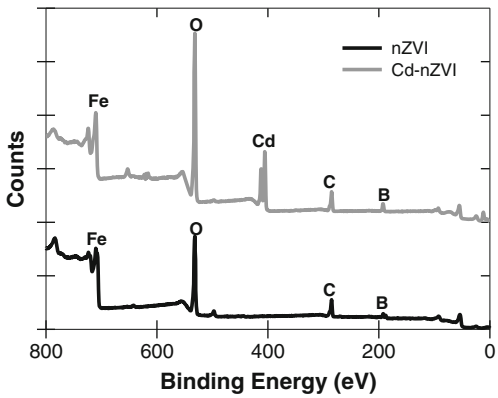

Fig. 4 Wide-scan XPS survey of fresh nZVI and Cd-nZVI after 72 h of reaction

The high-resolution Fe 2p spectrums of nZVI and Cd-nZVI indicate the presence of two iron components (Fig. 5b). A prominent peak at ~707 eV corresponding to the binding energy of $2p_{3/2}$ of zerovalent iron (Grosvenor et al. 2004b, c) indicates the presence of Fe^0 in the nZVI particles. The photoelectron peak for Fe^0 ($2p_{3/2}$) in the nZVI has also been reported earlier (Li et al. 2006; Li and Zhang 2007). The peaks at ~710 (Fe $2p_{3/2}$) and ~724 eV (Fe $2p_{1/2}$) are indicative of the oxidized iron species (Fe^{2+}/Fe^{3+}) which may be present as iron hydroxides ($Fe(OH)_x$), iron oxyhydroxide (FeOOH), or iron oxides (Fe_xO_y) (Grosvenor et al. 2004a; c). The peak at ~719 eV is composed of the shakeup satellite $2p_{3/2}$ for oxidized iron (Fe^{3+}) and $2p_{1/2}$ for Fe^0 (Grosvenor et al. 2004a; Li and Zhang 2007).

O 1s survey scans were conducted to study the oxygen species on nZVI and Cd-nZVI surfaces (Fig. 5c). The photoelectron peak for the O 1 s region decomposes into three peaks at 530, 531.9, and 533.2 eV, corresponding to the binding

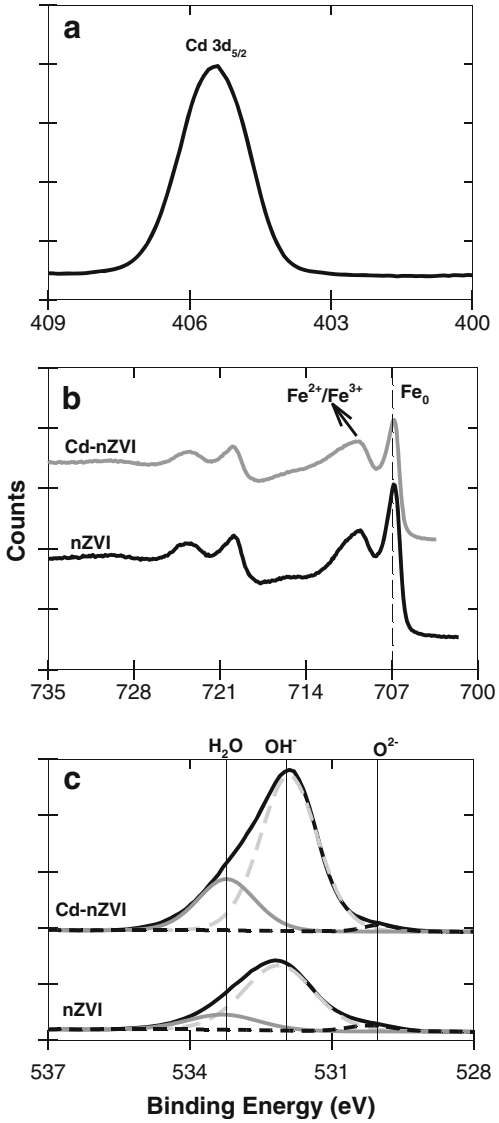

Fig. 5 High-resolution XPS surveys of **a** Cd 3d and **b** Fe 2p and **c** O 1 s of nZVI and Cd-nZVI

energies of O^{2-}, OH^-, and adsorbed water, respectively (Grosvenor et al. 2004b; Hanawa et al. 2002). The O^{2-} peak contributes less than 5 % of the total O 1s peak area in both nZVI and Cd-nZVI. This might be due to the very limited exposure of nZVI particles to oxygen/air as the nZVI synthesis, Cd adsorption, and XPS analysis were conducted under strictly anaerobic conditions. The OH^- peaks contributed 77.4 and 73.8 % of the total peak area in the nZVI and Cd-nZVI particles, respectively. This suggests the dominating iron species in the outer oxide layer to be iron hydroxides ($Fe(OH)_x$). Previous studies have also reported OH^- as the dominant peak in the O 1S region for nZVI (Li et al. 2006; Xi et al. 2010). Some researchers have reported the OH^-/O^{2-} ratio in nZVI to be ~1.0 (Li and Zhang 2006, 2007), whereas Manning et al. (2007) found O^{2-} as the dominant peak in the O 1s region of nZVI. The dominance of OH^- or O^{2-} in the O 1s region of iron metal is strongly influenced by the extent of its exposure to oxygen and water (Grosvenor et al. 2004b, c) which can vary depending upon the synthesis and handling of nZVI particles. The O 1s peak at ~530 eV assigned to iron oxides (Fe_xO_y) and at ~532 eV assigned to iron hydroxides ($Fe(OH)_x$) and iron oxyhydroxide (FeOOH) in studies characterizing iron and steel surfaces (Grosvenor et al. 2004a; Zabarskas et al. 2004) further support $Fe(OH)_x$ as the dominant species in the oxide layer of nZVI particles used in this study. The dominant $Fe(OH)_x$ species in the oxide layer might have favored greater Cd adsorption on nZVI (Dermatas and Meng 2004).

Effects of solution chemistry on cadmium adsorption by nZVI

Effect of adsorbent dosage

The adsorbent dosage strongly affects the metal removal efficiency of a system. When the nZVI dosage was increased from 0.1 to 5.0 g L^{-1}, the percent Cd removal increased from 22.5 % at 0.1 g L^{-1} to ~100 % at ≥0.5 g L^{-1} nZVI dosage (Fig. 6). This is due to the greater surface area and availability of more adsorption sites at higher dosages of the adsorbent. Although the cadmium removal percentage increased with increasing nZVI dosage, the metal uptake (i.e., the amount of Cd^{2+} adsorbed per unit mass of nZVI) decreased with increasing nZVI loading at higher nZVI dosages. The increase in metal uptake from 2.26 to 4.68 mmol g^{-1} with increase in nZVI dosage from 0.1 to 0.2 g L^{-1} can be attributed to greater availability and filling of adsorption sites at 0.2 g L^{-1}. The decrease in metal uptake thereafter may be attributed to the unsaturation/partial filling of sorption sites as the number of sorption sites increased with increase in nZVI content, but the amount of sorbate remained constant (i.e., the nZVI has not reached its adsorption capacity). As the difference in Cd removal percentage between 0.5 and 5.0 g nZVI L^{-1} was not significant, the nZVI loading of 0.5 g L^{-1} was selected for further studies.

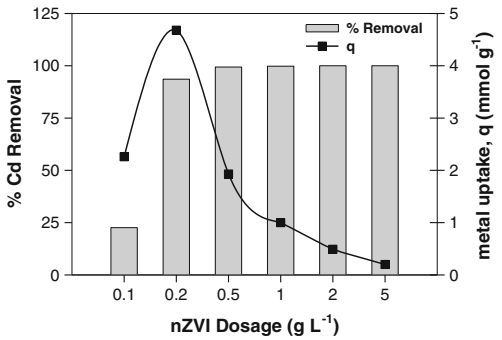

Fig. 6 Effect of nZVI dosage on cadmium adsorption by nZVI

Effect of initial cadmium concentration and contact time

Cadmium adsorption was significantly influenced by the initial concentration of cadmium in aqueous solutions. The percent Cd removal decreased from 100 to 80 % with increase in initial Cd^{2+} concentration from 0.25 to 4.0 mM (data not shown). At lower Cd^{2+} concentrations, the ratio of initial moles of Cd^{2+} to the available adsorption sites was low, and thus, complete adsorption occurred. However, at higher Cd^{2+} concentrations, the available adsorption sites decreased compared to the moles of Cd^{2+} present in the solution, and thus, the percentage sorption of metal decreased. The sorption capacities corresponding to equilibrium adsorption increased from 0.5 to 6.84 mmol g^{-1} with an increase in initial cadmium concentration (Fig. 7). This can be attributed to increasing driving force of the Cd^{2+} ions towards the adsorptive sites on nZVI surface (Kumar et al. 2010). The relationship between contact time and cadmium sorption onto nZVI particles at different initial cadmium concentrations is shown in Fig. 7. The adsorption was initially fast (i.e., first 12 h), decreased progressively with time, and finally approached equilibrium. The time to reach equilibrium varied according to the initial cadmium concentration (i.e., about 12 h for C_0=0.25 mM, 24 h for C_0=0.5 and 1.0 mM, and 48 h for C_0=2.0 and 4.0 mM). The initial fast adsorption might be due to the large amount of adsorptive sites available at the beginning; as the adsorption sites were gradually filled up, the adsorption became slower.

Effect of competitive cations

When two or more metal ions are present together in solution, they may increase (synergism), decrease (antagonism), or do not affect (non-interaction) the metal ion adsorption capacity of the system. Alkali and alkaline-earth metal cations such as Na^+, K^+, Mg^{2+}, and Ca^{2+} are commonly present with metal contaminants in polluted waters. Also, various heavy metal ions like Zn, Pb, Ni, Cu, and Mn co-exist with Cd at sites contaminated due to industrial applications and mining operations. Thus, it is necessary to study the competing effects of these metal ions on Cd^{2+} adsorption by nZVI. Cd adsorption onto nZVI decreased in the presence of other divalent metal ions (Fig. 8a). This is attributable to two effects: direct competition between the cations for sorption sites and the shielding effect of surface charge produced by competitive cations. However, the effect of competitive cations on cadmium sorption differed from metal to metal and was in the following order: $Zn^{2+}>Co^{2+}>Mg^{2+}>Mn^{2+}=Cu^{2+}>Ca^{2+}>Na^{+}=K^{+}$=Control. This varying antagonistic effect can be attributed to: (1) the different affinities of competitive cations for the binding sites and (2) the presence of different groups of binding sites on the adsorbent (Benjamin and Leckie 1981).

The properties of metal ions such as electronegativity, hydroxy complex formation ability, and the preference for specific sorption sites affect their affinity for the binding sites. The metals with higher electronegativities are adsorbed quickly by adsorbents such as metal (hydr)oxides and activated carbon (Mohapatra et al. 2010). As the metal-hydroxy species are sorbed preferentially over the metal ion, the metals with higher first hydrolysis constants may also affect the Cd^{2+} adsorption (Benjamin and Leckie 1981). Decreased adsorption of Cd^{2+} in the presence of Co^{2+} can be attributed to higher electronegativity and hydrolysis constant of Co^{2+} than Cd^{2+}. Due to its highest electronegativity

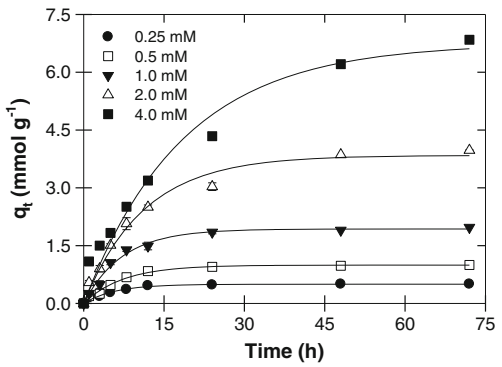

Fig. 7 Effect of initial Cd^{2+} concentration and contact time on cadmium adsorption by nZVI

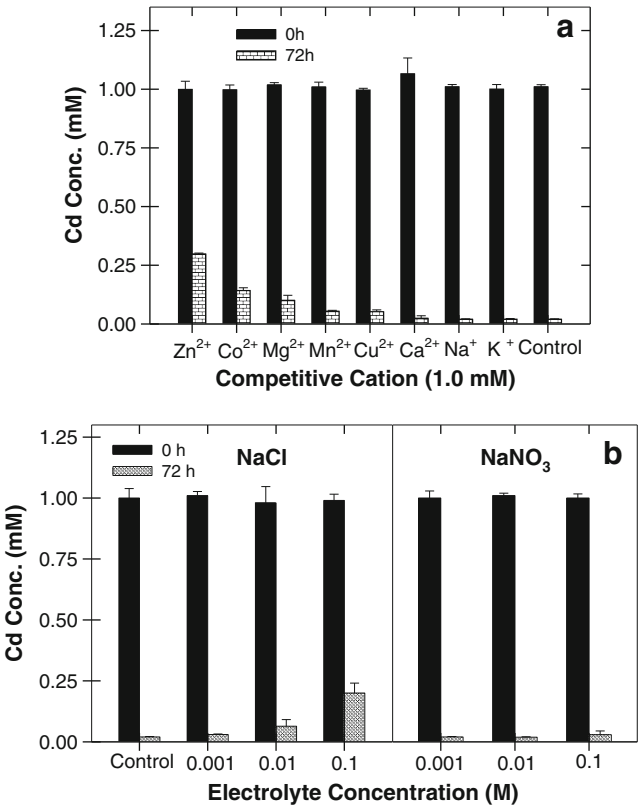

Fig. 8 Effect of **a** competitive cations and **b** ionic strength and electrolyte type on Cd^{2+} adsorption by nZVI

and hydrolysis constant, Cu^{2+} would be expected to compete strongly with Cd^{2+} for adsorption on nZVI, but this is not the case here. Cu^{2+}, with a highly positive redox potential (E^0=0.34), is mainly removed by reduction to Cu^{+} and Cu^{0} by nZVI (Li and Zhang 2007) and so may not compete for adsorption sites. Zn^{2+} has the most prominent effect with a 30 % decrease in Cd^{2+} adsorption onto nZVI. Due to the chemical similarities between Cd and Zn, they may strongly compete for the same adsorption sites (Utomo and Hunter 2006; Zasoski and Burau 1988). Tiller et al. (1979) reported that specifically sorbed Cd cannot be desorbed by Ca^{2+} but can be readily exchanged by another specifically sorbing ion such as Zn. This also suggests Cd^{2+} adsorption by nZVI to be a chemisorption (specific sorption) process. The low electronegativity and hydrolysis constant values of Ca^{2+}, Na^{+}, and K^{+} support their minimal effect on Cd^{2+} adsorption by nZVI. Moreover, each Cd^{2+} ion is sorbed on to two sorption sites on nZVI (Boparai et al. 2011) so Na^{+} and K^{+} (monovalent cations) may not compete with Cd^{2+} (divalent) for same adsorption sites.

Effect of ionic strength and electrolyte type

The effect of ionic strength on cadmium adsorption by nZVI helps in estimating the adsorption efficiency of nZVI in natural waters. It also helps in distinguishing between the inner- and outer-sphere complexation as adsorption mechanisms for metals (Dzombak and Morel 1990). The outer-sphere complexes are more sensitive to variations in ionic strength than are the inner-sphere complexes. The increase in $NaNO_3$ concentration from 0.001 to 0.1 M did not have any pronounced effect on Cd^{2+} adsorption (Fig. 8b). This further confirms the formation of inner-sphere complexes (chemisorption) between Cd^{2+} and nZVI. This also shows that there is no competitive effect of Na^{+} on Cd^{2+} adsorption by nZVI.

To study the effect of electrolyte type (inorganic anions) on Cd sorption by nZVI, NaCl was also used as an electrolyte. The amount of Cd^{2+} ions removed by nZVI decreased significantly with increase in the concentration of NaCl (Fig. 8b). This may be attributed to the presence of Cl^{-} in the system. Previous studies have shown that the presence of Cl^{-} ion reduced Cd sorption by various adsorbents due to the formation of Cd-Cl complexes, especially $CdCl^{+}$, which has a lower affinity for sorption compared with the divalent Cd^{2+} (Boekhold et al. 1993; Rao et al. 2011). Boekhold et al. (1993) also observed a much higher Cd sorption by soils in the presence of NO^{3-} than Cl^{-}.

Effect of pH

Aqueous phase pH strongly influences the adsorption process as it affects the surface charge of the adsorbent and the degree of ionization and speciation of the metal contaminant. Experiments were conducted over a pH range of 4 to 10 to study the effect of pH on Cd^{2+} adsorption onto nZVI. Cadmium removal by nZVI was highly pH-dependent, and the plot of % Cd adsorbed versus pH was sigmoidal (Fig. 9a). Cd removal was higher in the alkaline pH range (pH >7) and reached ~100 % at pH ≥8.0. The same trend of pH dependence of Cd adsorption has been reported for various other adsorbents (Balistrieri and Murray 1982; Benjamin and Leckie 1981; Unuabonah et al. 2008). In the highly acidic medium (pH <5), there is a possibility of nZVI dissolution and a consequent decrease in active adsorption sites. Moreover, a higher concentration of H^{+} ions in the solution at acidic pH may compete with Cd^{2+} for the adsorption sites, resulting in the reduced Cd^{2+} adsorption. The effect of pH on Cd sorption is also related to the changes in the surface charge and can be explained in terms of point of zero charge (pH_{pzc}). Below the pH_{pzc}, the adsorbent surface is protonated (Eq. 2), and an electrostatic repulsion exists between the positively charged surface and Cd^{2+} ions, inhibiting the adsorption. At pH above the pH_{pzc}, the nZVI surface acquires a net negative charge (Eq. 3) making the surface electrostatically favorable for higher adsorption of Cd^{2+}. In the present study, the pH_{pzc} of nZVI is 7.9, but most of the Cd^{2+} was adsorbed below this pH. This suggests that the nonspecific sorption (physisorption) due to electrostatic attractions between Cd^{2+} and nZVI surface is unlikely to be the major

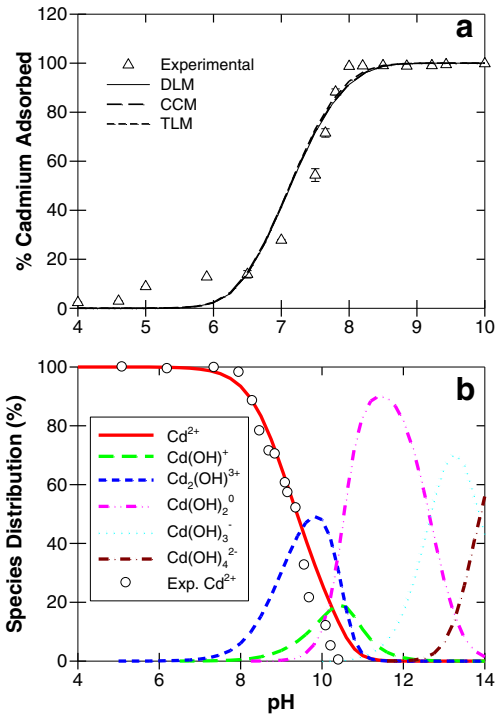

Fig. 9 **a** Effect of pH on Cd^{2+} adsorption by nZVI. *Lines* indicate the model fits using the three surface complexation models. **b** Cadmium speciation by Visual MINTEQ

mechanism for Cd^{2+} adsorption. This further supports that Cd^{2+} ions are adsorbed on the nZVI surface by specific sorption (chemisorption).

The other aspect to be considered is the metal speciation which is strongly influenced by pH and can affect the adsorption process. Speciation analysis of aqueous Cd^{2+} was performed using Visual MINTEQ. This analysis suggests that below pH 8.0 Cd is present nearly entirely as Cd^{2+} (Fig. 9b). However at pH ≥8.0, various Cd-hydroxy species start to form (i.e., $CdOH^+$, $Cd_2(OH)^{3+}$, $Cd(OH)_2{}^0$, $Cd(OH)_3{}^-$, and $Cd(OH)_4{}^{2-}$). Thus, at pH ≥8.0, cadmium hydrolysis/precipitation might have contributed to its removal from solution (Fig. 9a). The effect of pH on precipitation/hydrolysis of Cd^{2+} in aqueous solutions (without nZVI) was also studied experimentally. Cd^{2+} concentration started to decrease at pH 8.0 suggesting precipitation/hydrolysis to be contributing towards Cd^{2+} removal pH ≥8.0 (Fig. 9b). The model fit for Cd^{2+} was quite good with the model slightly overpredicting the amount of Cd^{2+} ions at pH ≥9.5.

Surface complexation modeling

Parameters used in the surface complexation modeling in this study are summarized in Table 2. The total site concentration (N_t) obtained from sorption isotherm data for Cd sorption onto nZVI at 24 °C was 6.84 mmol g^{-1} (Boparai et al. 2011). As the specific surface area of nZVI was 26.3 m^2 g^{-1}, this value corresponded to a site density (N_s) of 156.62 sites nm^{-2}. The surface ionization constants (Log K^+ or Log K^-) obtained by the single extrapolation method (Fig. 10) were applied to all the SCMs (Hayes et al. 1991). All the three surface complexation models, i.e., DLM, CCM, and TLM, showed a good fit for the Cd adsorption edge data (Fig. 9a). The respective $V(Y)$ values for these models were 2.57, 2.68, and 2.97. The values of $V(Y)$ between 0.1 and 20 indicate a good fit to the experimental data (Dzombak and Morel 1990). The good fit of DLM and CCM models suggests that the Cd^{2+} adsorption onto nZVI surface occurred via inner-sphere surface complexation. The presence of hydrolytic complexes considered in complexation equations of TLM did not make a significant difference to the model fit further supporting Cd^{2+} adsorption to be an inner-sphere complexation process. The relative concentrations of

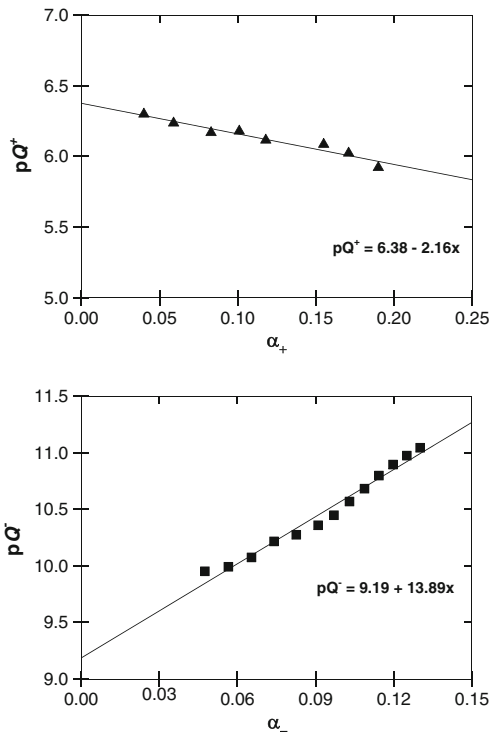

Fig. 10 Acidity quotient (pQ^+ or pQ^-) as a function of the fractional ionization of the surface

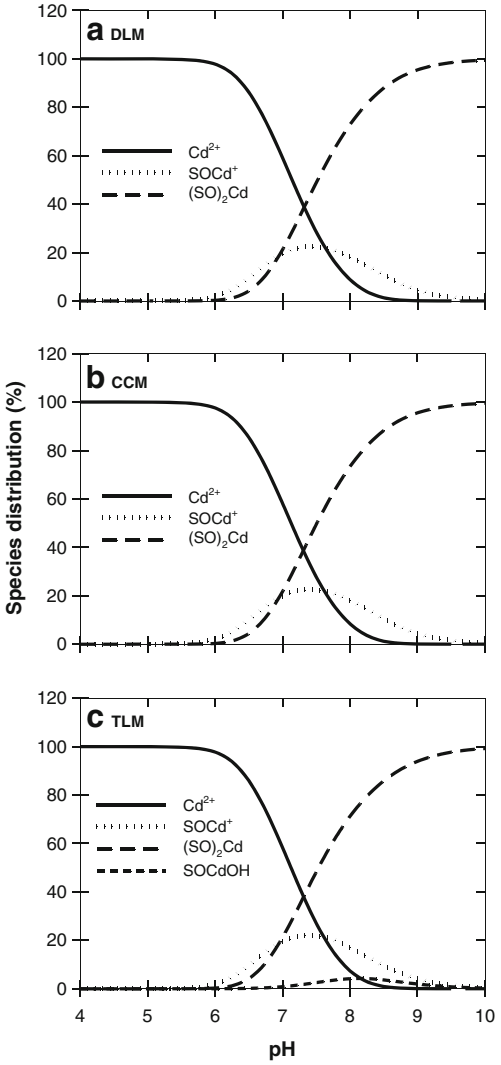

Fig. 11 Speciation diagram for Cd^{2+} adsorption on nZVI as calculated from the surface complexation models using the parameters from Table 2

various surface species (formed due to surface complexation of Cd^{2+} with nZVI surface) as a function of pH, calculated from the model parameters, are shown in Fig. 11. $(SO)_2Cd$ was found to be the dominant surface species for all the three models indicating the Cd^{2+} adsorption onto nZVI surface occurred via bidentate inner-sphere surface complexation. This is consistent with the pseudo second-order kinetics of Cd^{2+} adsorption on nZVI which suggested that one cadmium ion was adsorbed onto two sorption sites via chemisorption (Boparai et al. 2011).

Conclusions

nZVI can be used as an effective adsorbent for removing cadmium from contaminated water sources. EDX analysis showed that Cd was mainly distributed on the nZVI particles supporting adsorption as the mechanism for Cd removal. XPS results further confirmed the removal of Cd^{2+} ions by nZVI through adsorption. The dominant $OH_{(ads)}$ peak of the O 1 s region in nZVI suggested $Fe(OH)_x$ to be the dominating iron species in the oxide layer. Cadmium adsorption decreased in the presence of competitive cations in the order: $Zn^{2+}>Co^{2+}>Mg^{2+}>Mn^{2+}=Cu^{2+}>Ca^{2+}>Na^{2+}=K^{+}$. Ionic strength did not have any effect on Cd^{2+} sorption, but the presence of Cl^{-} ions at higher concentrations significantly decreased the Cd^{2+} sorption by nZVI. Cadmium removal increased with solution pH and reached 100 % at pH ≥8.0. The three surface complexation models: DLM, CCM, and TLM fitted well to the adsorption edge data. $(SO)_2Cd$ was the dominant surface species for all three models indicating the Cd^{2+} adsorption onto nZVI occurred via bidentate innersphere surface complexation. These results suggest that nZVI can be effectively used for the removal of cadmium from contaminated ground and surface water sources with a range of aqueous phase chemistries. Previous literature showing successful Cd^{2+} removal by various iron minerals suggests that the aqueous corrosion of nZVI with time resulting in the formation of iron (hydr)oxides can facilitate further continuous adsorption of Cd^{2+}. nZVI has become a promising technology for remediating groundwater and can be quite successful for mixed waste (organic and metal contaminants) sites. Information related to Cd removal by nZVI is helpful in effectively employing this technology at the mixed waste sites.

Acknowledgments This research was supported by the EJLB foundation, Natural Sciences and Engineering Research Council (NSERC) of Canada, and Canadian Foundation for Innovation Grant. We would like to thank Mark Biesinger, Qing Mu, and Ross Davison for the XPS and SEM/EDX analysis as well as Clare Robinson for her assistance with the speciation modelling.

References

ATSDR (2008) ToxFAQs™ for cadmium. Agency for Toxic Substances and Disease Registry, Atlanta, GA. http://www.atsdr.cdc.gov/tfacts5.pdf. Accessed 30 Nov 2012

ATSDR (2011) Detailed data table for the 2011 priority list of hazardous substances that will be the subject of toxicological profiles. Agency for Toxic Substances and Disease Registry, Atlanta, GA. http://www.atsdr.cdc.gov/SPL/resources/ATSDR_2011_SPL_Detailed_Data_ Table.pdf. Accessed 30 Nov 2012

Balistrieri LS, Murray JW (1982) The adsorption of Cu, Pb, Zn, and Cd on goethite from major ion sea-water. Geochim Cosmochim Acta 46:1253–1265. doi:10.1016/0016-7037(82)90010-2

Benguella B, Benaissa H (2002) Effects of competing cations on cadmium biosorption by chitin. Colloid Surf A 201:143–150. doi:10.1016/S0927- 7757(01)00899-8

Benjamin MM, Leckie JO (1981) Competitive adsorption of Cd, Cu, Zn, and Pb on amorphous iron oxyhydroxide. J Colloid Interf Sci 83:410–419. doi:10.1016/0021-9797(81)90337-4

Boekhold AE, Temminghoff EJM, Vanderzee SEATM (1993) Influence of electrolyte-composition and pH on cadmium sorption by an acid sandy soil. J Soil Sci 44:85–96. doi:10.1111/j.1365-2389.1993.tb00436.x

Boparai HK, Joseph M, O'Carroll DM (2011) Kinetics and thermodynamics of cadmium ion removal by adsorption onto nano zerovalent iron particles. J Hazard Mater 186:458–465. doi:10.1016/j.jhazmat.2010.11.029

Bose DN, Hedge MS, Basu S, Mandal KC (1989) XPS investigation of Cdte surfaces—effect of Ru modification. Semicond Sci Tech 4:866–870. doi:10.1088/0268-1242/4/10/006

Calareso C, Grasso V, Silipigni L (2001) The cadmium seleniophosphate (CdPSe3) XPS and XAES spectra. Appl Surf Sci 171:306–313. doi:10.1016/S0169-4332(00)00818-7

Celebi O, Uzum C, Shahwan T, Erten HN (2007) A radiotracer study of the adsorption behavior of aqueous Ba^{2+} ions on nanoparticles of zero-valent iron. J Hazard Mater 148:761–767. doi:10.1016/j.jhazmat.2007.06.122

Davis JA, James RO, Leckie JO (1978) Surface ionization and complexation at oxide/water interface. 1. Computation of electrical double-layer properties in simple electrolytes. J Colloid Interf Sci 63:480–499. doi:10.1016/S0021-9797(78)80009-5

Dermatas D, Meng X (2004) Removal of As, Cr and Cd by adsorptive filtration. Global Nest J 6:73–80

Dinis ML, Fiuza A (2011) Exposure assessment to heavy metals in the environment: measures to eliminate or reduce the exposure to critical receptors. In: Simeonov LI, Kochubovski MH, Simeonova BG (eds) Environmental heavy metal pollution and effects on child mental development. Springer, Dordrecht, pp 27–50

Dzombak DA, Morel FMM (1990) Surface complexation modeling: hydrous ferric oxide. Wiley Inter Science, New York

Efecan N (2008) Characterization of the adsorption behaviour of aqueous Cd(II) and Ni(II) ions on nanoparticles of zero-valent iron. M.S. Thesis. İzmir Institute of Technology, Turkey

Efecan N, Shahwan T, Eroglu AE, Lieberwirth I (2009) Characterization of the uptake of aqueous Ni^{2+} ions on nanoparticles of zero-valent iron (nZVI). Desalination 249:1048–1054. doi:10.1016/j.desal.2009.06.054

Fairley N (1999) CasaXPS Version 2.2.19. www.casaxps.com

Good NE, Izawa S (1972) Hydrogen ion buffers. Method Enzymol 24:53–68. doi:10.1016/0076-6879(72)24054-X

Grosvenor AP, Kobe BA, Biesinger MC, McIntyre NS (2004a) Investigation of multiplet splitting of Fe 2p XPS spectra and bonding in iron compounds. Surf Interface Anal 36:1564–1574. doi:10.1002/sia.1984

Grosvenor AP, Kobe BA, McIntyre NS (2004b) Studies of the oxidation of iron by air after being exposed to water vapour using

angle-resolved X-ray photoelectron spectroscopy and QUASES. Surf Interface Anal 36:1637–1641. doi:10.1002/sia.1992

Grosvenor AP, Kobe BA, McIntyre NS (2004c) Studies of the oxidation of iron by water vapour using X-ray photoelectron spectroscopy and QUASES (TM). Surf Sci 572:217–227. doi:10.1016/j.susc.2004.08.035

Gustafsson JP (2011) Visual MINTEQ version 3.0 [Online]. Department of Land and Water Resources Engineering, Royal Institute of Technology, Stockholm, Sweden. http://www.lwr.kth.se/English/OurSoftware/vminteq/. Accessed 22 Oct 2012

Hanawa T, Hiromoto S, Yamamoto A, Kuroda D, Asami K (2002) XPS characterization of the surface oxide film 316 L stainless steel samples that were located in quasi-biological environments. Mater Trans 43:3088–3092

Hayes KF, Redden G, Ela W, Leckie JO (1991) Surface complexation models—an evaluation of model parameter-estimation using FITEQL and oxide mineral titration data. J Colloid Interf Sci 142:448–469. doi:10.1016/0021-9797(91)90075-J

Huang QY, Chen WL, Xu LH (2005) Adsorption of copper and cadmium by Cu- and Cd-resistant bacteria and their composites with soil colloids and kaolinite. Geomicrobiol J 22:227–236. doi:10.1080/01490450590947779

Kanel SR, Manning B, Charlet L, Choi H (2005) Removal of arsenic(III) from groundwater by nanoscale zero-valent iron. Environ Sci Technol 39:1291–1298. doi:10.1021/Es048991u

Kanel SR, Greneche JM, Choi H (2006) Arsenic(V) removal from groundwater using nano scale zero-valent iron as a colloidal reactive barrier material. Environ Sci Technol 40:2045–2050. doi:10.1021/Es0520924

Kumar PS, Ramakrishnan K, Kirupha SD, Sivanesan S (2010) Thermodynamic and kinetic studies of cadmium adsorption from aqueous solution onto rice husk. Braz J Chem Eng 27:347–355. doi:10.1590/S0104-66322010000200013

Li XQ, Elliott DW, Zhang WX (2006) Zero-valent iron nanoparticles for abatement of environmental pollutants: materials and engineering aspects. Crit Rev Solid State 31:111–122. doi:10.1080/10408430601057611

Li XQ, Zhang WX (2006) Iron nanoparticles: the core–shell structure and unique properties for Ni(II) sequestration. Langmuir 22:4638–4642. doi:10.1021/La060057k

Li XQ, Zhang WX (2007) Sequestration of metal cations with zerovalent iron nanoparticles—a study with high resolution X-ray photoelectron spectroscopy (HR-XPS). J Phys Chem C 111:6939–6946. doi:10.1021/Jp0702189

Lindsay WL (1979) Chemical equilibria in soils. Wiley, New York

Manning BA, Kiser JR, Kwon H, Kanel SR (2007) Spectroscopic investigation of Cr(III)- and Cr(VI)-treated nanoscale zerovalent iron. Environ Sci Technol 41:586–592. doi:10.1021/Es061721m

Mohapatra M, Mohapatra L, Singh P, Anand S, Mishra BK (2010) A comparative study on Pb(II), Cd(II), Cu(II), Co(II) adsorption from single and binary aqueous solutions on additive assisted nano-structured goethite. Int J Eng, Sci Technol 2(8):89–103. http://www.ajol.info/index.php/ijest/article/view/63784

Mondal K, Jegadeesan G, Lalvani SB (2004) Removal of selenate by Fe and NiFe nanosized particles. Ind Eng Chem Res 43:4922–4934. doi:10.1021/ie0307151

Moreno-Castilla C, Alvarez-Merino MA, Lopez-Ramon MV, Rivera-Utrilla J (2004) Cadmium ion adsorption on different carbon adsorbents from aqueous solutions. Effect of surface chemistry, pore texture, ionic strength, and dissolved natural organic matter. Langmuir 20:8142–8148. doi:10.1021/La049253m

O'Carroll D, Sleep B, Krol M, Boparai H, Kocur C (2012) Nanoscale zerovalent iron and bimetallic particles for contaminated site remediation. Adv Water Resour In Press. doi:10.1016/j.advwatres.2012.02.005

Petersen EJ, Pinto RA, Shi X, Huang Q (2012) Impact of size and sorption on degradation of trichloroethylene and polychlorinated biphenyls by nano-scale zerovalent iron. J Hazard Mater 243:73–79. doi:10.1016/j.jhazmat.2012.09.070

Rao KS, Anand S, Venkateswarlu P (2011) Adsorption of cadmium from aqueous solution by *Ficus religiosa* leaf powder and characterization of loaded biosorbent. Clean-Soil Air Water 39:384–391. doi:10.1002/clen.201000098

Sakulchaicharoen N, O'Carroll DM, Herrera JE (2010) Enhanced stability and dechlorination activity of pre-synthesis stabilized nanoscale FePd particles. J Contam Hydrol 118:117–127. doi:10.1016/j.jconhyd.2010.09.004

Satapanajaru T, Anurakpongsatorn P, Pengthamkeerati P, Boparai H (2008) Remediation of atrazine-contaminated soil and water by nano zerovalent iron. Water Air Soil Poll 192:349–359. doi:10.1007/s11270-008-9661-8

Schaller MS, Koretsky CM, Lund TJ, Landry CJ (2009) Surface complexation modeling of Cd(II) adsorption on mixtures of hydrous ferric oxide, quartz and kaolinite. J Colloid Interf Sci 339:302–309. doi:10.1016/j.jcis.2009.07.053

Soltani RDC, Jafari AJ, Khorramabadi GS (2009) Investigation of cadmium (II) ions biosorption onto pretreated dried activated sludge. Am J Environ Sci 5:41–46. doi:10.3844/ajes.2009.41.46

Song H, Carraway ER (2005) Reduction of chlorinated ethanes by nanosized zero-valent iron: kinetics, pathways, and effects of reaction conditions. Environ Sci Technol 39:6237–6245. doi:10.1021/Es048262e

Tiller KG, Nayyar VK, Clayton PM (1979) Specific and nonspecific sorption of cadmium by soil clays as influenced by zinc and calcium. Aust J Soil Res 17:17–28. doi:10.1071/SR9790017

Üzüm Ç, Shahwan T, Eroğlu AE, Lieberwirth I, Scott TB, Hallam KR (2008) Application of zero-valent iron nanoparticles for the removal of aqueous Co^{2+} ions under various experimental conditions. Chem Eng J 144:213–220. doi:10.1016/j.cej.2008.01.024

Unuabonah EI, Adebowale KO, Olu-Owolabi BI, Yang LZ, Kong LX (2008) Adsorption of Pb(II) and Cd(II) from aqueous solutions onto sodium tetraborate-modified kaolinite clay: equilibrium and thermodynamic studies. Hydrometallurgy 93:1–9. doi:10.1016/j.hydromet.2008.02.009

Utomo HD, Hunter KA (2006) Adsorption of divalent copper, zinc, cadmium and lead ions from aqueous solution by waste tea and coffee adsorbents. Environ Technol 27:25–32. doi:10.1080/09593332708618619

Xi YF, Mallavarapu M, Naidu R (2010) Reduction and adsorption of Pb^{2+} in aqueous solution by nano-zero-valent iron—an SEM, TEM and XPS study. Mater Res Bull 45:1361–1367. doi:10.1016/j.materresbull.2010.06.046

Yan S, Hua B, Bao Z, Yang J, Liu C, Deng B (2010) Uranium(VI) removal by nanoscale zerovalent iron in anoxic batch systems. Environ Sci Technol 44:7783–7789. doi:10.1021/es9036308

Zabarskas V, Tamulevicius S, Prosycevas I, Puiso J (2004) Analysis of Fe_3O_4 protective coatings thermally grown on color picture TV tube structural steel components. Mater Sci-Medzg 10(2):147–151. http://internet.ktu.lt/lt/mokslas/zurnalai/medz/pdf/medz0-77/05%20Zabarsko%20str%20147-151.pdf

Zalups RK, Ahmad S (2003) Molecular handling of cadmium in transporting epithelia. Toxicol Appl Pharmacol 186:163–188. doi:10.1016/S0041-008x(02)00021-2

Zasoski RJ, Burau RG (1988) Sorption and sorptive interaction of cadmium and zinc on hydrous manganese oxide. Soil Sci Soc Am J 52:81–87

Zhang L, Manthiram A (1997) Chains composed of nanosize metal particles and identifying the factors driving their formation. Appl Phys Lett 70:2469–2471

Zhang W-x (2003) Nanoscale iron particles for environmental remediation: an overview. J Nanopart Res 5:323–332. doi:10.1023/A:1025520116015

Zhu NR, Luan HW, Yuan SH, Chen J, Wu XH, Wang LL (2010) Effective dechlorination of HCB by nanoscale Cu/Fe particles. J Hazard Mater 176:1101–1105. doi:10.1016/j.jhazmat.2009.11.092